Organic Nonlinear Optical Crystals Based on Configurationally Locked Polyene for Melt Growth

O-Pil Kwon,*,† Blanca Ruiz,† Ashutosh Choubey,† Lukas Mutter,† Arno Schneider,† Mojca Jazbinsek,† Volker Gramlich,‡ and Peter Günter†

Nonlinear Optics Laboratory and Laboratory of Crystallography, ETH Zurich, CH-8093 Zurich, Switzerland

Received May 2, 2006

A series of nonlinear optical chromophores based on configurationally locked polyene are synthesized, and the single crystal growth from the melt are investigated. The chromophores consist of a π-conjugated hexatriene bridge between the dialkylamino or methoxy electron donors and the dicyanomethylidene electron acceptor. The physical and nonlinear optical properties and the single crystal X-ray structures of these chromophores are characterized. Specifically, the chromophore 2-{3-[2-(4-dimethylaminophenyl)-vinyl]-5,5-dimethylcyclohex-2-enylidene}malononitrile (DAT2) exhibits a strong powder second-harmonic generation signal of about 2 orders of magnitude greater than that of urea and a large temperature difference of 80 °C between the melting temperature and the recrystallization temperature. Finally, we demonstrate the growth of single crystalline thin films of DAT2 by a Bridgman-type melt growth technique, which gives a new direction for organic nonlinear optical crystal engineering using melt−growth techniques.

Introduction

Organic nonlinear optical materials have received considerable attention as a result of numerous potential applications in photonics and relatively high and fast nonlinearities compared to their inorganic counterparts.[1] The long-term orientational stability of nonlinear optical molecules in crystals is significantly superior to those of polymers because of spontaneous acentric arrangement of the molecules eliminating the need for poling as in polymers. Nonlinear optical organic crystals are very promising for terahertz (THz) generation and detection[2] and for the development of broadband integrated photonic devices, such as microresonator filters and modulators.[3] Although they have superior stability compared to poled polymers, organic nonlinear optical crystals are typically difficult to process, especially in thin films that are needed for the development of structures compatible with microelectronic processing.[4] Therefore, there is a strong interest to develop new organic nonlinear optical materials with better processing possibilities as nowadays state-of-the-art materials, for example, 4′-(dimethylamino)-*N*-methyl-4-stilbazolium tosylate (DAST)[5] that exhibits large nonlinear optical susceptibility and electrooptic coefficient[6] but an insufficient thermal stability for melt growth.

Solution growth techniques for organic nonlinear optical crystals are most common but limited to rather low growth rates (in many cases $\sim$ 0.1−1 mm/day) and solvent or solution inclusion problems.[1] Melt growth techniques on the other hand do not possess these restrictions. However, growth from the solution represents in many cases the only possibility of obtaining single crystals due to insufficient thermal stability of the organic molecules to apply melt growth techniques. Usually the melt growth cannot be applied for long π-conjugated chromophores with high melting temperature due to the long-term thermal instability at the growth temperature which is in most cases near the melting temperature T_m. Therefore, the short π-conjugated chromophores with relatively low melting temperature (T_m < 150 °C) and also short wavelength of absorption maximum (λ_{max} < 400 nm) such as mNA, NPP, MAP, COANP, and others were the only organic nonlinear optical crystals obtained by melt growth techniques up to now.[1] Additionally, thin platelet crystals (quasi two-dimensional) are naturally more compatible with planar waveguide configurations compared to bulk crystals (three-dimensional), leading to a high confinement of optical waves in photonic devices. A single crystalline film forming in a short period of time by a melt growth

* To whom correspondence should be addressed. Fax: +41 1 633 1056. Tel.: +41 1 633 3258. E-mail: kwon@phys.ethz.ch.
† Nonlinear Optics Laboratory.
‡ Laboratory of Crystallography.

(1) (a) Bosshard, Ch.; Bösch, M.; Liakatas, I.; Jäger, M.; Günter, P. In *Nonlinear Optical Effects and Materials*; Günter, P., Ed.; Springer-Verlag: Berlin, 2000; Chapter 3. (b) Bosshard, Ch.; Sutter, K.; Prêtre, Ph.; Hulliger, J.; Flörsheimer, M.; Kaatz, P.; Günter, P. *Organic Nonlinear Optical Materials*; *Advances in Nonlinear Optics*; Gordon and Breach Science Publishers: Langhorne, PA, 1995; Vol. 1. (c) Nalwa, H. S.; Watanabe, T.; Miyata, S. In *Nonlinear Optics of Organic Molecules and Polymers*; Nalwa, H. S., Miyata, S., Eds.; CRC Press: Boca Raton, FL, 1997; Chapter 4.

(2) (a) Schneider, A.; Biaggio, I.; Günter, P. *Appl. Phys. Lett*. **2004**, *84*, 2229. (b) Taniuchi, T.; Ckada, S.; Nakanishi, H. *J. Appl. Phys*. **2004**, *95*, 5984.

(3) Jazbinsek, M.; Rabiei, P.; Bosshard, Ch.; Günter, P. *AIP Conf. Proc.* **2004**, *709*, 187.

(4) (a) Geis, W.; Sinta, R.; Mowers, W.; Deneault, S. J.; Marchant, M. F.; Krohn, K. E.; Spector, S. J.; Calawa, D. R.; Lyszczarz, T. M. *Appl. Phys. Lett*. **2004**, *84*, 3729. (b) Kaino, T.; Cai, B.; Takayama, K. *Adv. Funct. Mater*. **2002**, *12*, 599. (c) Kutty, S. P.; Thakur, M. *Appl. Phys. Lett*. **2005**, *87*, 191111.

(5) (a) Marder, S. R.; Perry, J. W.; Yakymyshyn, C. P. *Chem. Mater*. **1994**, *6*, 1137. (b) Pan, F.; Wong, M. S.; Bosshard, Ch.; Günter, P. *Adv. Mater*. **1996**, *8*, 592.

(6) Pan, F.; Knöpfle, G.; Bosshard, Ch.; Follonier, S.; Spreiter, R.; Wong, M. S.; Günter, P. *Appl. Phys. Lett*. **1996**, *69*, 13.

10.1021/cm0610130 CCC: $33.50
Published on Web 07/29/2006

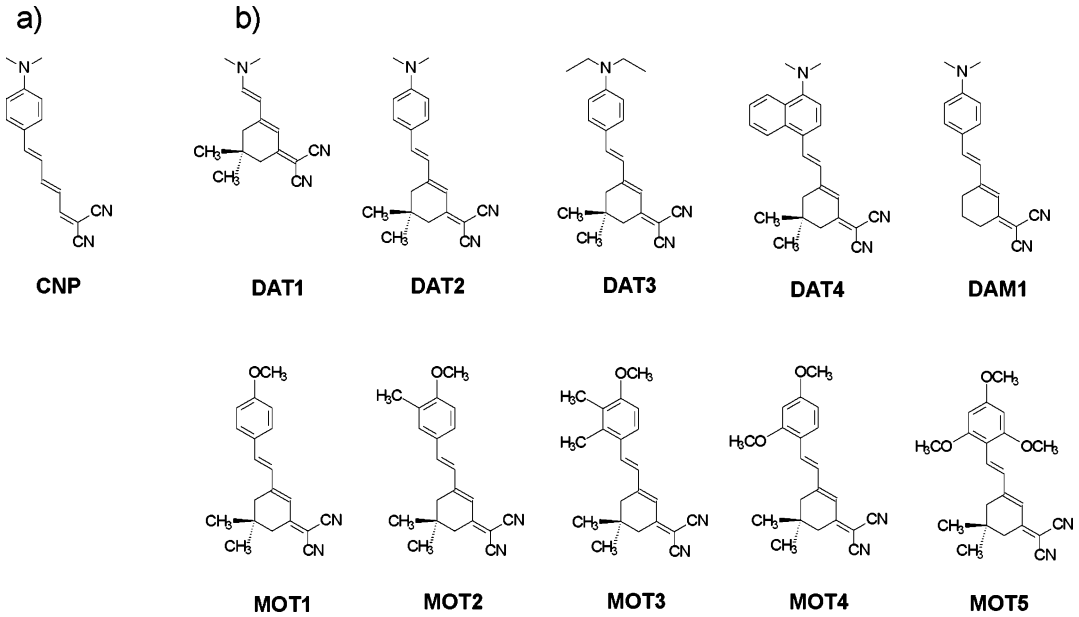

Figure 1. Chemical structures of CNP (a) and investigated CLP (b) chromophores.

technique would be, therefore, for many photonic devices much more attractive than a bulk crystal grown by the traditional solution growth.

The macroscopic second-order nonlinear optical response d_{333} (and similarly r_{333}) is related to the corresponding microscopic molecular hyperpolarizability β and the structural parameters N and θ_p as follows: $d_{333} = N\beta f(\omega)\langle\cos^3\theta_p\rangle$, where N is number of molecules per unit volume, $f(\omega)$ is the local field factor, and θ_p is the angle between the molecular charge-transfer axis and the polar crystalline axis.[1] Therefore, for obtaining a crystal with a large second-order nonlinear optical activity, the constituting molecules should possess large microscopic molecular hyperpolarizability β and crystallize in a noncentrosymmetric arrangement. Molecular engineering for acentric arrangement of polar organic chromophores in crystals is still a challenging topic because of the high tendency of nonlinear optical chromophores to form the antiparallel dipole−dipole aggregation.[7] Moreover, it is the preliminary step to crystal growth engineering and integration of the material to the final device.

To obtain a large molecular second-order nonlinearity the long conjugated polyene chromophores provide one of the most effective pathways for efficient charge delocalization between donor and acceptor groups without loss of the aromaticity.[8] However, the thermal and photochemical instability for conventional nonlocked polyene (CNP, Figure 1a) chromophores limits growth engineering in the melt growth technique, that is, the so-called nonlinearity−thermal stability tradeoff. Therefore, a major challenge in designing the nonlinear optical chromophores is to simultaneously achieve acceptable thermal stability, transparency, nonlinearity, and processability in one compound. Recently, several chromophores with the polyene chain incorporated into a ring system have been developed to improve thermal and photochemical stability.[9−12] To evade the nonlinearity−thermal stability tradeoff for the melt growth, we here synthesize and investigate a series of 10 different configurationally locked polyene (CLP) chromophores. These consist of a π-conjugated hexatriene bridge between dialkylamino or methoxy donors and a dicyanomethylidene acceptor. We characterize the physical and nonlinear optical properties and structures of the chromophores and their crystals by X-ray diffraction. Finally, we demonstrate the growth of single crystalline thin films of DAT2 crystals by a Bridgman-type melt growth technique.

Experimental Section

Synthesis and General Characterization. The various CLP chromophores were synthesized by two consecutive Knoevenagel condensations. The intermediates were prepared by the condensation of 3,5,5-trimethyl-2-cyclohexen-1-on (isophorone) or 3-methyl-2-cyclohexen-1-on with malononitrile using ammonium acetate and were then used for the second condensation with *N*,*N*-dimethylformamide dimethylacetal for DAT1 or the corresponding donor

(7) (a) Yang, Z.; Aravazhi, S.; Schneider, A.; Seiler, P.; Jazbinsek, M.; Günter, P. *Adv. Funct. Mater.* **2005**, *15*, 1072. (b) Sliwa, M.; Letard, S.; Malfant, I.; Nierlich, M.; Lacroix, P. G.; Asahi, T.; Masuhara, H.; Yu, P.; Nakatani, K. *Chem. Mater.* **2005**, *17*, 4727. (c) Nesterov, V. V.; Antipin, M. Y.; Nesterov, V. N.; Moore, C. E.; Cardelino, B. H.; Timofeeva, T. V. *J. Phys. Chem. B* **2004**, *108*, 8531. (d) Floc'h, V. L.; Brasselet, S.; Zyss, J.; Cho, B. R.; Lee, S. H.; Jeon, S. J.; Cho, M.; Min, K. S.; Suh, M. P. *Adv. Mater.* **2005**, *17*, 196. (e) Coe, B. J.; Harris, J. A.; Asselberghs, I.; Wostyn, K.; Clays, K.; Persoons, A.; Brunschwig, B. S.; Coles, S. J.; Gelbrich, T.; Light, M. E.; Hursthouse, M. B.; Nakatani, K. *Adv. Funct. Mater.* **2003**, *13*, 347. (f) Srinivas, K.; Sitha, S.; Rao, V. J.; Bhanuprakash, K.; Ravikumar, K.; Anthony, S. P.; Radhakrishnan, T. P. *J. Mater. Chem.* **2005**, *15*, 965.

(8) (a) Marder, S. R.; Beratan, D. N.; Cheng, L. T. *Science* **1991**, *252*, 103. (b) Marder, S. R.; Cheng, L. T.; Tiemann, B. G.; Friedli, A. C.; Blanchare-Desce, M.; Perry, J. W.; Skindhoj, J. *Science* **1994**, *263*, 511.

(9) Shu, C. F.; Tsai, W. J.; Jen, A. K.-Y. *Tetrahedron Lett.* **1996**, *37*, 7055.

(10) Ermer, S.; Lovejoy, S. M.; Leung, D. S.; Warren, H.; Moylan, C. R.; Twieg, R. J. *Chem. Mater.* **1997**, *9*, 1437.

(11) (a) Shu, C. F.; Shu, Y. C.; Gong, Z. H.; Peng, S. M.; Lee, G. H.; Jen, A. K.-Y. *Chem. Mater.* **1998**, *10*, 3284. (b) Shu, Y. C.; Gong, Z. H.; Shu, C. F.; Breitung, E. M.; McMahon, R. J.; Lee, G. H.; Jen, A. K.-Y. *Chem. Mater.* **1999**, *11*, 1628.

(12) (a) Staub, K.; Levina, G. A.; Barlow, S.; Kowalczyk, T. C.; Lackritz, H. S.; Barzoukas, M.; Fort, A.; Marder, S. R. *J. Mater. Chem.* **2003**, *13*, 825. (b) Lawrentz, U.; Grahn, W.; Lukaszuk, K.; Klein, C.; Wortmann, R.; Feldner, A.; Scherer, D. *Chem.—Eur. J.* **2002**, *8*, 1573.

containing aldehyde using piperidine according to the literature.[10,13] All chemicals were obtained from commercial suppliers (Aldrich). ^{1}H NMR spectra were recorded on a Varian 300 MHz. The chemical shifts are reported in ppm (δ) relative to $(CH_3)_4Si$. UV−vis absorption spectra were recorded by a Perkin-Elmer Lambda 9 spectrometer. Thermal measurements were carried out using Perkin-Elmer TGA-7 and DSC-7 spectrometer (10 °C/min scan rate).

DAT1. ^{1}H NMR ($CDCl_3$, δ): 7.08 (d, 1H, −CH═CH−), 6.38 (s, 1H, −C═CH−), 5.26 (d, 1H, −CH═CH−), 3.0 (s, 6H, N−CH_3), 2.47 (s, 2H, −CH_2), 2.26 (s, 2H, −CH_2), 1.0 (s, 6H, −CH_3).

DAT2. ^{1}H NMR ($CDCl_3$, δ): 7.4 (d, 2H, Ar−H), 7.0 (d, 1H, −CH═CH−), 6.8 (d, 1H, −CH═CH−), 6.75 (s, 1H, −C═CH−), 6.7 (d, 2H, Ar−H), 3.0 (s, 6H, N−CH_3), 2.6 (s, 2H, −CH_2), 2.5 (s, 2H, −CH_2), 1.0 (s, 6H, −CH_3).

DAT3. ^{1}H NMR ($CDCl_3$, δ): 7.4 (d, 2H, Ar−H), 7.0 (d, 1H, −CH═CH−), 6.8 (d, 1H, −CH═CH−), 6.73 (s, 1H, −C═CH−), 6.6 (d, 2H, Ar−H), 3.4 (q, 4H, N−CH_2−), 2.57 (s, 2H, −CH_2), 2.45 (s, 2H, −CH_2), 1.2 (t, 6H, −CH_3), 1.0 (s, 6H, −CH_3).

DAT4. ^{1}H NMR ($CDCl_3$, δ): 7.0−8.3 (m, 6H, Ar−H), 7.03 and 7.84 (two d, 1H each, −CH═CH−), 6.86 (s, 1H, −C═CH−), 2.96 and 2.93 (two s, 6H, N−CH_3), 2.63 (s, 2H,-CH_2), 2.6 (s, 2H, −CH_2), 1.13 (s, 6H, −CH_3).

DAM1. ^{1}H NMR ($CDCl_3$, δ): 7.4 (d, 2H, Ar−H), 7.0 (d, 1H, −CH═CH−), 6.8 (d, 1H, −CH═CH−), 6.75 (s, 1H, −C═CH−), 6.7 (d, 2H, Ar−H), 3.0 (s, 6H, N−CH_3), 2.76 (t, 2H, −CH_2), 2.63 (t, 2H, −CH_2), 1.9 (m, 2H, −CH_2).

MOT1. ^{1}H NMR ($CDCl_3$, δ): 7.6 (d, 2H, Ar−H), 7.0 (d, 1H, −CH═CH−), 6.92 (d, 2H, Ar−H), 6.89 (d, 1H, −CH═CH−), 6.8 (s, 1H, −C═CH−), 3.85 (s, 3H, O−CH_3), 2.6 (s, 2H, −CH_2), 2.46 (s, 2H, −CH_2), 1.0 (s, 6H, −CH_3).

MOT2. ^{1}H NMR ($CDCl_3$, δ): 7.34 (s and d, 2H, Ar−H), 7.0 (d, 1H, −CH═CH−), 6.88 (d, 1H, −CH═CH−), 6.84 (d, 1H, Ar−H), 6.8 (s, 1H, −C═CH−), 3.87 (s, 3H, O−CH_3), 2.6 (s, 2H, −CH_2), 2.46 (s, 2H, −CH_2), 1.0 (s, 6H, −CH_3).

MOT3. ^{1}H NMR ($CDCl_3$, δ): 6.3−7.5 (m, 5H, Ar−H and −CH═CH−), 6.8 (s, 1H, −C═CH−), 3.85 (s, 3H, O−CH_3), 2.6 (s, 2H, −CH_2), 2.5 (s, 2H, −CH_2), 2.3 (s, 3H, −CH_3), 2.2 (s, 3H, −CH_3), 1.0 (s, 6H, −CH_3).

MOT4. ^{1}H NMR ($CDCl_3$, δ): 7.5 (d, 1H, Ar−H), 7.34 (d, 1H, −CH═CH−), 6.89 (d, 1H, −CH═CH−), 6.78 (s, 1H, −C═CH−), 6.54 (m, 1H, Ar−H), 6.46 (d, 1H, Ar−H), 3.89 and 3.85 (each s, 6H, O−CH_3), 2.6 (s, 2H, −CH_2), 2.4 (s, 2H, −CH_2), 1.0 (s, 6H, −CH_3).

MOT5. ^{1}H NMR ($CDCl_3$, δ): 7.45 (d, 1H, −CH═CH−), 6.78 (s, 1H, −C═CH−), 6.6−6.3 (m, 1H, −CH═CH−), 6.13 (s, 2H, Ar−H), 3.9−3.7 (three s each, 9H, O−CH_3), 2.6 (s, 2H, −CH_2), 2.4 (s, 2H, −CH_2), 1.0 (s, 6H, −CH_3).

EFISH Experiments. For the measurements of the $\mu_g\beta_z$ values electric field induced second-harmonic generation (EFISH) measurements were performed as described in ref 14 with pulses at the wavelength 1907 nm that were generated by focusing light of a Q-switched Nd:YAG laser (λ = 1064 nm, repetition rate 10 Hz, pulse duration 25 ns) into a Raman cell filled with a 25 bar H_2 pressure. Voltage pulses of 30 μs durations were applied to the wedged cell, generating a static field of around 11 kV/cm. As a reference, a 1% 2-methyl-4-nitroaniline (MNA) dioxane solution was used with a macroscopic third-order nonlinearity $\Gamma = 9.14 \times 10^{-22}$ m^2/V^2,[14] which was measured with a quartz reference having a second-order nonlinear optical coefficient $d_{11} = 0.277$ pm/V.[14,15] All measurements were performed with chloroform as the solvent. For the analysis of the measurements the extrapolation procedure to infinite dilution was used as derived from Singer and Garito[16] applying the perturbation convention of ref 17. Because chloroform is a polar solvent, Onsager local field factors for static frequencies and Debye type for optical frequencies were taken into account for the determination of the ground-state dipole moment μ_g and the hyperpolalizability β_z values.

Powder Second-Harmonic Generation (SHG) Measurements. For the Kurtz and Perry powder test[18] we used a tunable output of an optical parametric amplifier pumped by an amplified Ti:sapphire laser. Typical pulse energy and durations were 50 μJ and 150 fs (full width at half-maximum), respectively. Experiments at a fundamental wavelength of 1.3 μm were done with the parametric signal wave. The backscattered light at the second-harmonic wavelength (650 nm) was measured with a silicon photodiode that is not sensitive to the fundamental wavelength becaues of the absorption edge of Si near 1.1 μm. The diode signal was averaged over 100 pulses and integrated with a digital oscilloscope. Contributions from third-harmonic generation (450 nm for a fundamental wavelength of 1.3 μm) were eliminated using appropriate filters.

X-ray Crystal Structures. Single crystal X-ray diffraction experiments of CLP derivatives were carried out on a single crystal X-ray diffractometer equipped with a charge-coupled device detector (Xcalibur PX, Oxford Diffraction) with a 65 mm sample−detector distance. Data reduction and numerical absorption were performed using the software package CrysAlis.[19] The crystal structures were solved by direct methods, and the full data sets were refined on F^2, employing the programs SHELXS-97 and SHELXL-97.[20] Crystallographic data (excluding structure factors) for the structure(s) reported in this paper have been deposited with the Cambridge Crystallographic Data Center as supplementary publication no. CCDC-278086 (DAT1), CCDC-278087 (DAT2), CCDC-278088 (DAT3), CCDC-278090 (DAT4), CCDC-278089 (DAM1), CCDC-278091 (MOT1 with active SHG), CCDC-278092 (MOT1 with inactive SHG), CCDC-278093 (MOT2), and CCDC-278094 (MOT3). Copies of the data can be obtained free of charge via www.ccdc.cam.ac.uk/conts/retrieving.html.

Results and Discussion

Synthesis and Characterization. The chemical structures of investigated CLP chromophores in this study are shown in Figure 1b together with their abbreviations. The various CLP chromophores were synthesized by two consecutive Knoevenagel condensations according to the literature.[10,13] The chemical structures of all compounds were confirmed by ^{1}H NMR results. The donors are various dialkylamino groups or more than one methoxy group. The configurationally locked triene was a link between the donors and the dicyanomethylidene [>C═C(CN)$_2$] acceptor. To increase the thermal stability and the tendency for inducing an acentric packing, a structurally asymmetric group of the cyclohexene ring and/or steric substituents by the two methyl groups in the hexatriene bridge were incorporated into the chromophores.

(13) Chun, H.; Moon, I. K.; Shin, D. H.; Kim, N. *Chem. Mater*. **2001**, *13*, 2813.
(14) Bosshard, Ch.; Knöpfle, G.; Prêtre, P.; Günter, P. *J. Appl. Phys*. **1992**, *71*, 1594.
(15) Eckardt, R. C.; Masuda, H.; Fan, Y. X.; Byer, R. L. *IEEE J. Quantum Electron*. **1990**, *26*, 922.
(16) Singer, K. D.; Garito, A. F. *J. Chem. Phys*. **1991**, *75*, 3572.
(17) Willetts, A.; Rice, J. E.; Burland, D. M.; Shelton, D. P. *J. Chem. Phys*. **1992**, *97*, 7590.
(18) Kurtz, S. K.; Perry, T. T. *J. Appl. Phys*. **1968**, *39*, 3798.
(19) http://www.oxford-diffraction.com.
(20) (a) Sheldrick, G. *SHELXS-97; Program for the Solution of Crystal Structures*; University of Göttingen: Göttingen, Germany, 1997. (b) Sheldrick, G. *SHELXL-97; Program for the Refinement of Crystal Structures*; University of Göttingen: Göttingen, Germany, 1997.

Table 1. Results of Physical, Chemical, and Structural Measurements of the Investigated CLP Chromophore Derivatives[a]

	T_m (°C)	T_c (°C)	T_d (°C)	λ_{max} (nm)	μ_g (10^{-29} C m)	β_z (10^{-40} m^4 V^{-1})	crystal system	point group	space group
DAT1	205	160	275	482	4.08	200	triclinic	$\bar{1}$	$P\bar{1}$
DAT2	235	155	293	502	3.21	1100	monoclinic	2	$P2_1$
DAT3	174	N[b]	313	518	3.46	1050	monoclinic	$2/m$	$P2_1/c$
DAT4	216	N	307	459	2.64	590	triclinic	$\bar{1}$	$P\bar{1}$
DAM1	218	193	290	498	3.24	1010	orthorhombic	*mmm*	*Pnma*
MOT1[c]	124	N	290	422	2.69	340	orthorhombic monoclinic	222 $2/m$	$P2_12_12_1$ $P2_1/c$
MOT2	199	N	293	427	2.72	420	monoclinic	$2/m$	$P2_1/n$
MOT3	180	N	293	418	2.48	310	monoclinic	$2/m$	$C2/c$
MOT4	171	N	311	435	2.96	480			
MOT5	211	168	292	440	3.29	400			

[a] T_d, decomposition temperature; T_m, melting temperature, T_c, recrystallization temperature; λ_{max}, wavelength of the maximum absorption in chloroform solution; μ_g, ground state dipole moment; and β_z, second-order polarizability measured at 1907 nm by EFISH. [b] N means that the chromophores did not exhibit recrystallization in the cooling scan at a scan rate of 10 °C/min. [c] The structure of two polymorphs is given for MOT1; the orthorhombic phase exhibits second-harmonic activity.

The results of the physical characteristics, including the thermal properties, absorption properties, ground-state dipole moment μ_g, molecular hyperpolarizability β_z, and crystal system are summarized in Table 1. The microscopic nonlinear optical property $\mu_g\beta_z$ was determined by EFISH measurements at the wavelength 1907 nm in chloroform using a Q-switched Nd:YAG laser into a Raman cell filled with a 25 bar H_2 pressure.[14] From the measured ground-state dipole moment μ_g the values of the second-order hyperpolarizability β_z were evaluated. The wavelength of maximum absorption λ_{max} for the CLP chromophores is in the range of 418−518 nm in chloroform. The charge-transfer bands show a stronger red shift with increased donor strength (dialkylamino > methoxy). The molecular hyperpolarizability β_z from EFISH measurement for CLP chromophores exhibits a similar behavior, as expected.[1] The β_z values for CLP chromophores with the phenylhexatriene bridge show a strong correlation with the absorption maximum (λ_{max}), leading to the so-called nonlinearity−transparency tradeoff from the two-level model of the sum-over-states method for nonlinear optical chromophores.[1] The dependence of β_z as a function of λ_{max} for the investigated chromophores plotted in a double logarithmic scale is close to linear $\beta \propto \lambda^x$ with a slope $x = 6.0 \pm 0.5$.

Powder SHG Measurements. The Kurtz and Perry powder test[18] was used to qualitatively screen the CLP derivatives at a fundamental wavelength of 1.3 μm using an optical parametric amplifier pumped by an amplified Ti:sapphire laser. We compare the powder second-harmonic activity of the nonionic CLP crystals to the ionic crystals of DAST that present one of the best organic materials for second-order nonlinear optics (1000 times higher second-harmonic signal than that of urea at 1.9 μm).[5] Two crystalline powders of DAT2 and MOT1 chromophores exhibited very strong SHG signals of 35 and 14% of that of DAST, respectively.

X-ray Crystal Structures. Single crystals suitable for X-ray diffraction analysis for all the CLP chromophores were grown from methanol solution. Saturated solutions of each chromophore in methanol were prepared at 40 °C. The containers were kept at constant temperature for 2 days to fully saturate and stabilize the solution. We found that cooling the solutions to room temperature in most cases did not produce spontaneous nucleation, and, therefore, it was necessary to induce crystallization with a drastic change in the vapor pressure of the container at 40 °C to room temperature. After nucleation we allowed the crystals to grow for one more day, and then we removed them from the solution.

Table 2. Summary of Crystallographic Data for the Acentric DAT2 Crystal and MOT1 Crystal

	DAT2	MOT1
powder SHG[a]	35%	14%
formula	$C_{21}H_{23}N_3$	$C_{20}H_{20}N_2O$
formula weight	317.42	304.38
crystal system	monoclinic	orthorhombic
space group	$P2_1$	$P2_12_12_1$
a (Å)	6.1303(7)	5.7242(4)
b (Å)	7.4239(9)	7.5711(6)
c (Å)	20.258(4)	40.258(2)
α (deg)	90	90
β (deg)	96.750(8)	90
γ (deg)	90	90
V (Å^3)	915.6(2)	1744.7(2)

[a] Powder SHG measured at a fundamental wavelength of 1.3 μm relative to that of DAST powder.

The obtained crystal point and space groups as determined by X-ray crystallography are given in Table 1. The DAT2 and MOT1 crystals have noncentrosymmetric structures, monoclinic with space group symmetry $P2_1$ (point group 2), and orthorhombic with a space group symmetry $P2_12_12_1$ (point group 222), respectively. Therefore, for second-order nonlinear optical applications, the DAT2 and MOT1 crystals appear to be the most attractive ones. We, therefore, investigated these crystals in more detail and included the details about the crystallographic structure (Table 2) in this paper.

Figure 2 shows the molecular arrangement of DAT2 projected along the c axis of the crystal. In the DAT2 molecule, the phenyl ring and donor groups are planar. The double bond in the hexene ring and dicyanomethylidene acceptor are also planar but lie slightly out of the phenyl ring plane at an angle of 8.5°. The long axis of the DAT2 molecules, which is a favorable direction of charge delocalization, is aligned at an angle of $\theta_p = 71°$ relative to the polar b axis (order parameter $\cos\theta_p = 0.33$). This nonoptimal crystal packing with high molecular nonlinearity of DAT2 molecules results in a smaller macroscopic nonlinearity compared to that of DAST; however, in the powder test it still shows a high SHG signal of 35% of DAST as a result of the large hyperpolarizability of DAT2 molecule.

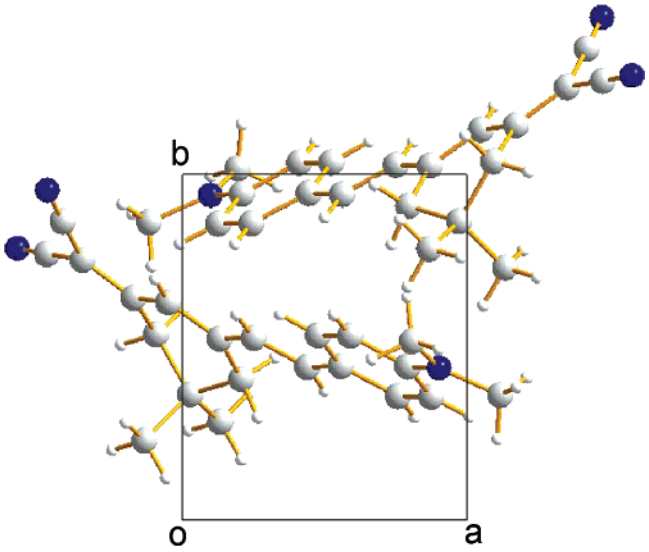

Figure 2. Crystal packing diagram projected along the *c* axis for the $P2_1$ phase of DAT2 with the twofold rotation axis along the polar *b* axis.

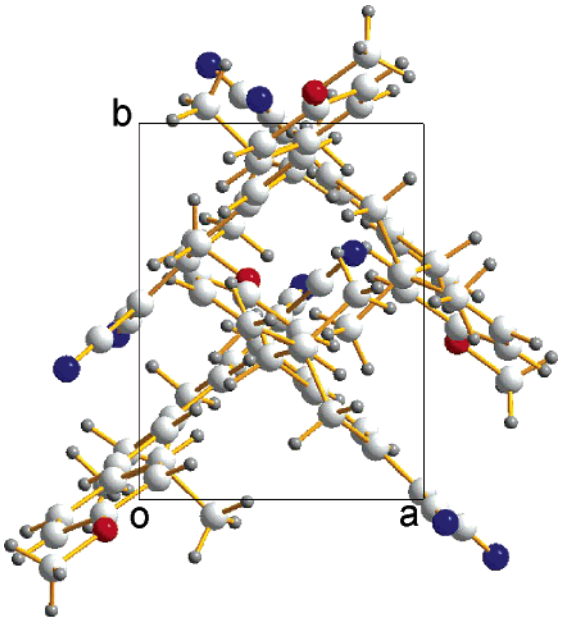

Figure 3. Crystal packing diagram projected along the *c* axis for the $P2_12_12_1$ phase of MOT1.

The MOT1 crystal is orthorhombic having a space group symmetry $P2_12_12_1$ (point group 222). The crystal structure is shown in Figure 3. The space group $P2_12_12_1$ is noncentrosymmetric but nonpolar. Therefore, the largest hyperpolalizability component β_{zzz} along the direction of the molecular dipole moment in the MOT1 molecules does not contribute to the macroscopic nonlinear susceptibilities. The main contribution to the macroscopic nonlinear optical susceptibilities in the MOT1 crystals is, therefore, due to other smaller hyperpolarizability components. Therefore, the powder test shows a smaller macroscopic nonlinearity of MOT1 compare to that of DAT2 (see Table 2).

Thermal Properties. The relative thermal stabilities of CLP chromophores were investigated using thermogravimetric analysis (TGA) and differential scanning calorimetry (DSC) under a nitrogen atmosphere at a scan rate of 10 °C/min. The decomposition temperature T_d was estimated as the temperature that is the intercept of the leading edge of the weight loss by the baseline of the TGA scans. The melting temperature T_m and the recrystallization temperature T_c were defined here as the ending point of the endothermic transition in the heating DSC scan and the starting point of the exothermic transition in the cooling DSC scan, respectively. The results of these measurements are given in Table 1 and are shown in Figure 4 for DAT2 and MOT1. Although the decomposition temperature T_d results not only from the decomposition but also from sublimation after melting, all of the CLP chromophores with the phenylhexatriene bridge exhibit large a T_d of over 290 °C, while for the CNP chromophore with the phenyltriene bridge the decomposition temperature of around 250 °C has been reported.[11,12] Therefore, a large temperature difference between the decomposition temperature T_d and the melting temperature T_m is expected to be a benefit for applying melt growth techniques.

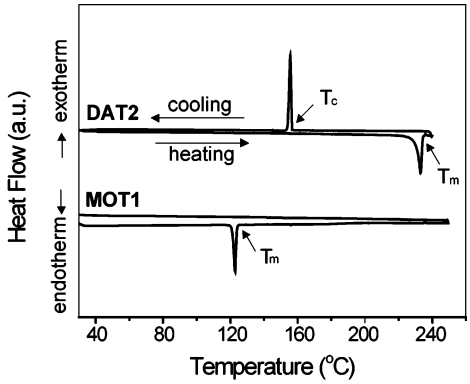

Figure 4. DSC curves of the DAT2 and MOT1 chromophore showing the melting temperature T_m and the recrystallization temperature T_c (scan rate: 10 °C/min).

The DAT2 chromophore with the dimethylamino donor group reveals two transitions in the DSC scan: melting (T_m) and recrystallization (T_c), whereas the MOT1 chromophore with a methoxy donor group does not show recrystallization in the cooling scan at a scan rate of 10 °C/min (see Figure 4). The melting temperature T_m and the recrystallization temperature T_c for the DAT2 chromophore appear at about 235 °C and about 155 °C, respectively. As seen in Figure 4, the starting point of recrystallization for DAT2 from the melt is very far from the melting temperature T_m ($\Delta T = T_m - T_c \approx 80$ °C). For the melt growth a large ΔT is also quite an important parameter. In the conventional melt growth technique the sample should be kept for a long time near the melting temperature T_m because of a slow translation rate of the materials in a furnance with a temperature gradient (1 mm/h or less) or a small supercooling (usually less than few degrees).[1] The large ΔT between the melting temperature T_m and the recrystallization temperature T_c for the DAT2 chromophore may give new possibilities for the growth engineering of organic crystals applying melt growth techniques.

Melt Crystal Growth. On the basis of the large difference between the melting and the decomposition temperatures and between the melting and the recrystallization temperatures for DAT2, we set up an experiment for the melt growth using a Bridgman-type configuration. The DAT2 molecule was put

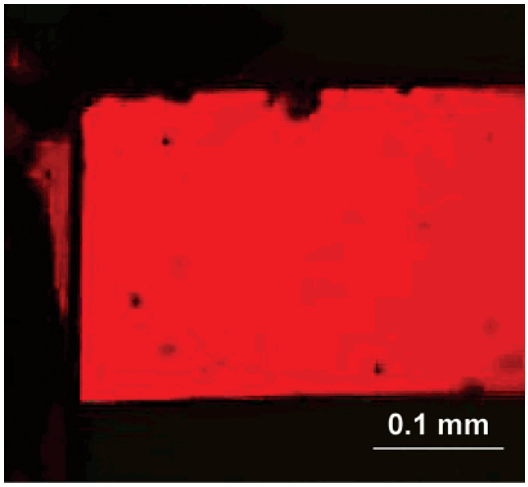

Figure 5. DAT2 thin film crystal grown from the melt as observed between crossed polarizers in a polarizing microscope.

into a quartz ampule and sealed with Ar gas at normal atmosphere pressure. The tube was placed inside a vertical furnace with the temperature gradient of 10 °C/cm between the hot (235 °C) and the cold (150 °C) zones. The ampule position was kept fixed, and the furnace was moved up vertically by 1.8 mm/h over the ampule. Hence, the ampule passed through the hot zone to the cold zone of the furnace. The DAT2 chromophore inside the ampule gets melted as it passes through the hot zone and then crystallizes as it passes through the cold zone of the furnace. After the crystals were grown, the ampule was cooled to room temperature with a cooling rate of 20 °C/h. On the wall of the ampule, platelet crystals of the DAT2 chromophore were obtained. Figure 5 shows one crystal grown by the above method as observed between the crossed polarizers in a microscope. The light transmission through the crystal homogeneously changes from transparent to opaque in the whole crystal region as the crystal is rotated around the direction of the light propagation, meaning that the crystal is single crystalline. Typically the crystals grown by the above method are in the shape of rectangular plates with side lengths in the range of 0.5−2 mm and thicknesses of less than about 50 μm. This shows that single crystalline thin films of the DAT2 chromophore of good quality can be grown by melt growth techniques. Future studies will focus also on modifying the chromophore structures further to optimize the noncentrosymmetric packing into the crystal structure.

Conclusion

We investigated the molecular nonlinear optical and thermal properties, the crystal growth, and the crystal packing of a series of the CLP chromophores based on the π-conjugated hexatriene bridge between dialkylamino or methoxy donors and the dicyanomethylidene acceptor. The CLP chromophores exhibit relatively high thermal stabilities with decomposition temperatures T_d above 290 °C. Two chromophores, DAT2 and MOT1, possess noncentrosymmetric structures. The DAT2 crystal exhibits very strong SHG signals of about 2 orders of magnitude greater than that of urea and reveals a large temperature difference of 80 °C between the melting temperature and the recrystallization temperature, favorable for applying melt growth techniques for obtaining the crystals. The single crystalline thin films of the DAT2 chromophore have been demonstrated by a Bridgman-type melt growth technique, which gives a new direction for organic nonlinear optical crystal engineering using melt growth techniques.

Acknowledgment. This work has been supported by the Swiss National Foundation. The authors are very grateful to Ms. S. J. Kwon for her synthetic support and Mr. R. Gianotti for his technical support.

CM0610130